

Fabrication of Gold Nanoparticles and Cinnamaldehyde-Functionalized Paper-Based Films and Their Antimicrobial Activities against White Film-Forming Yeasts

Seong Youl Lee, Eun Hae Kim, Tae-Woon Kim, Young-Bae Chung, Ji-Hee Yang, Sung Hee Park, Mi-Ai Lee, and Sung Gi Min*



Cite This: *ACS Omega* 2023, 8, 8256–8262



Read Online

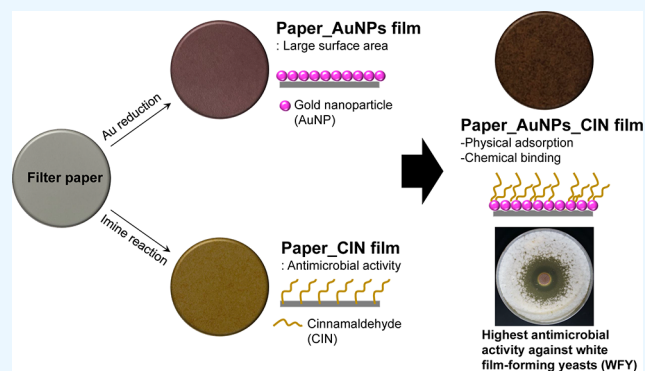
ACCESS |

Metrics & More

Article Recommendations

ABSTRACT: During storage and fermentation of kimchi, white film-forming yeasts (WFY) are generated on the surface of kimchi under various conditions. These yeasts include *Candida sake*, *Pichia kudriavzevii*, *Kazachstania servazzii*, *Debaryomyces hansenii*, and *Hanseniaspora uvarum*. Because of the off-odor and texture-softening properties of WFY that degrade the quality of kimchi, a method to prevent WFY is required. In this study, cinnamaldehyde (CIN) and gold nanoparticles (AuNPs) with a large surface area were grafted on a paper surface, which was termed the “Paper_AuNPs_CIN” film. CIN is an antimicrobial agent that is approved for use in food applications. In the as-fabricated Paper_AuNPs_CIN film, antimicrobial CIN molecules were physically adsorbed to the surface of AuNPs and simultaneously chemically synthesized on the paper surface via the imine reaction.

The Paper_AuNPs_CIN film exhibited greater antimicrobial activity against the three WFY strains than a Paper_CIN film (which contains only CIN molecules). Since more CIN molecules were adsorbed to the large surface area of the paper-reduced AuNPs, the Paper_AuNPs_CIN film exhibited a higher antimicrobial activity. Using AuNPs and CIN simultaneously to inhibit the growth of WFY is a novel approach that has not yet been reported. The morphology and elemental mapping of the functionalized films were examined via scanning electron microscopy and energy-dispersive spectroscopy, elemental composition was analyzed via inductively coupled plasma optical emission spectroscopy, and chemical bonding and optical properties were investigated via Fourier transform infrared spectroscopy and diffuse reflectance spectroscopy. Additionally, agar-well diffusion assays were used to determine the antimicrobial activity against three representative WFY strains: *C. sake*, *P. kudriavzevii*, and *K. servazzii*.



1. INTRODUCTION

Kimchi, one of the most well-known fermented foods, is fermented by microorganisms present in the various ingredients used to produce kimchi.¹ However, when white film-forming yeasts (WFY) are generated during fermentation, consumers are dissatisfied due to the off-odor and softened texture of kimchi.^{2,3} Since all products containing WFY during the storage of kimchi must be discarded, it is necessary to find ways to prevent the growth of WFY to avoid the commercial value of kimchi from deteriorating. According to storage conditions such as temperature, pH, and anaerobic conditions of kimchi, five types of WFY exist, including *Candida sake*, *Pichia kudriavzevii*, *Kazachstania servazzii*, *Debaryomyces hansenii*, and *Hanseniaspora uvarum*. Among these, antimicrobial experiments have been conducted on three representative strains previously.³

Cinnamaldehyde (CIN) has been widely used in the food preservation industry because of its antimicrobial properties

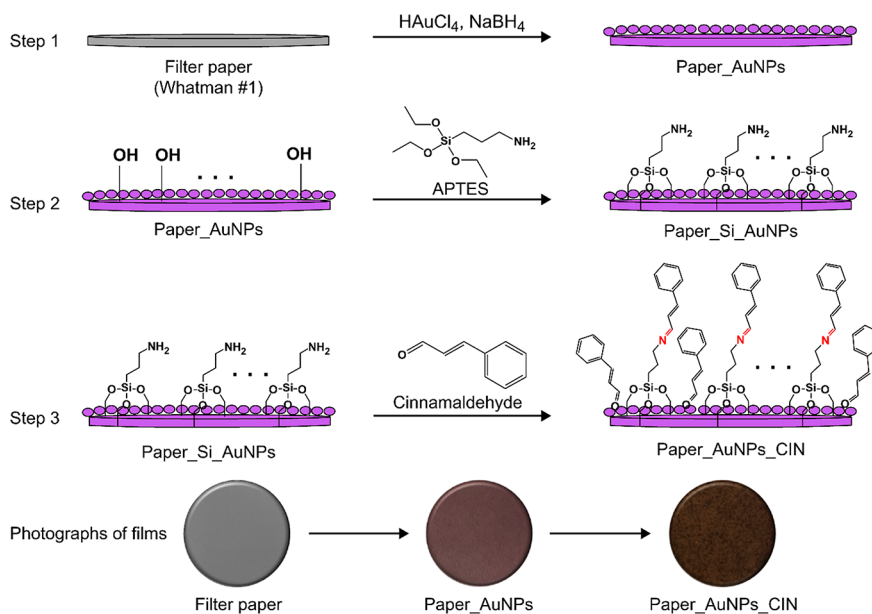
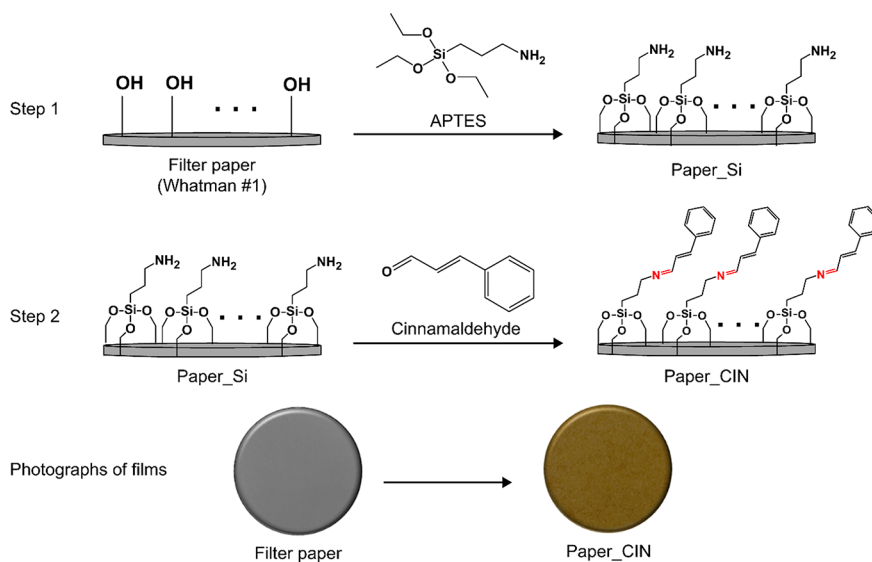
and the fact that it is nontoxic and approved by the U.S. Food and Drug Administration (FDA).⁴ Antimicrobial activities of CIN against gram-positive bacteria, gram-negative bacteria, and pathogenic yeast species have been reported in previous studies.⁵ However, CIN is difficult to use due to its poor aqueous solubility and potent odor, which affects the sensory properties of foods.⁶ Several candidates that inhibit the growth of WFY using CIN have been reported previously.^{7,8} In the cases where the CIN extract was sprayed directly onto the surface of kimchi, it was discovered that the more CIN was

Received: September 30, 2022

Accepted: December 30, 2022

Published: February 21, 2023



Scheme 1. Fabrication and Color-Change Photographs of the Paper Sample after Each Fabrication Step, as Labeled on the Scheme**Scheme 2. Fabrication and Color-Change Photographs of the Paper Sample without CIN (Left) and with CIN (Right)**

used to increase the antimicrobial activity, the more the scent of CIN affected the kimchi's sensory properties. To address this issue, a novel method was developed that preserves antimicrobial activity without affecting the sensory properties of contacted food, which was achieved through chemical bonding whereby the CIN molecules were bound to the film surface via the imine reaction.⁹

Gold nanoparticles (AuNPs) have garnered significant attention from researchers because of their unique size and surface properties compared to the bulk form and because they are widely functionalized for antimicrobial agents.^{10,11} Owing to their characteristics such as inertness, biocompatibility, and ease of functionalization, AuNPs are regarded as effective surface functionalization materials and were employed in this study. Meanwhile, paper has attracted interest as an eco-friendly material for packaging and medical devices, among other applications, because of its low cost and relative

abundance.¹² Accordingly, in this study, AuNPs were generated on the surface of paper, to take advantage of their larger surface area. Consequently, it was anticipated that the antimicrobial activities would be maximized by physically adsorbing more CIN molecules to the film surface by utilizing the adsorption affinity between AuNPs and CIN molecules.¹³

Herein, CIN, a naturally derived material, and AuNPs, which are inert in the biological environment, were incorporated onto the surface of paper to prepare an effective agent for inhibiting microbial growth against WFY. Since more CIN molecules are present on the surface owing to their adsorption with AuNPs than when CIN is bound solely by chemical bonding, the maximum antimicrobial activity can be expected. The functionalized films were characterized by scanning electron microscopy (SEM), inductively coupled plasma optical emission spectroscopy (ICP-OES), Fourier transform infrared spectroscopy (FT-IR), and diffuse reflectance spectroscopy

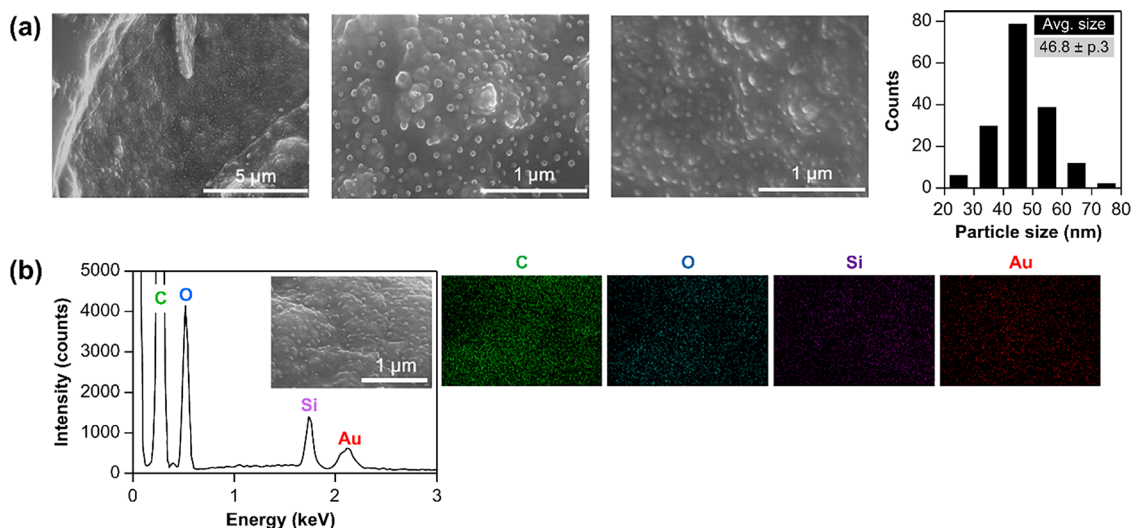


Figure 1. (a) SEM images of the Paper_AuNPs_CIN film and particle-size distribution of AuNPs; (b) the corresponding EDS spectrum and elemental mapping.

(DRS). Additionally, the antimicrobial properties of functionalized films were evaluated against WFY strains using an agar-well diffusion assay. To the best of our knowledge, this is the first study to fabricate a film using AuNPs and CIN and to test the antimicrobial activity of these two materials against WFY affecting kimchi.

2. METHODS

2.1. Fabrication of Paper_AuNPs_CIN and Paper_CIN Films. For Paper_AuNPs_CIN, 1 mL of 10 mM HAuCl_4 (99.9%, MERCK) ethanol solution was poured over a sheet of Whatman #1 filter paper (47 mm in diameter) and dried in a convection oven at 60 °C for 1 h (Scheme 1). The paper containing Au ions was then immersed in 5 mL of a 10 mM sodium borohydride (NaBH_4 , MERCK) aqueous solution for an additional hour. Au ions settled on the filter paper were reduced to AuNPs via a reduction reaction with NaBH_4 , resulting in an instantaneous color change from white to purple. The paper containing the AuNPs, labeled Paper_AuNPs, was then rinsed with deionized water and ethanol to remove any residual reagents and dried in a convection oven at 60 °C. The Paper_AuNPs film was submerged in 10 mL of toluene containing 5% 3-aminopropyltriethoxysilane (APTES, 99%, MERCK) and placed in a 30 °C, 100 rpm, shaking incubator for 1 day. The paper was then rinsed with toluene and dried in a convection oven to remove any residual APTES; it was then labeled as Paper_Si_AuNPs. The Paper_Si_AuNPs were then immersed in 10 mL of ethanol containing 5% *trans*-cinnamaldehyde (CIN, 99%, MERCK) and placed in a 50 °C, 100 rpm incubator for 1 day. The Paper_AuNPs_CIN film was fabricated by connecting amine groups on the outer surface of the Paper_Si_AuNPs film to *trans*-cinnamaldehyde (CIN, 99%, MERCK) via an imine ($\text{C}=\text{N}$) bond. The fabrication of Paper_AuNPs_CIN was completed by a drying procedure following three 5 min ultrasonication treatments with ethanol. The paper CIN was produced using the identical method without AuNPs reduction (Scheme 2).

2.2. Characterization of Various Functionalized Papers. The structures and surface morphologies of the functionalized papers image were obtained using SEM (Thermo Fisher Scientific, Verios 5 UC) after platinum

coating for 120 s. Additionally, energy-dispersive spectroscopy and elemental mapping (EDS, Oxford Instruments, AztecLive, and Ultim Max 65) were used in conjunction with SEM to determine the major atoms (C, O, Si, and Au) and atomic percentage of Paper_AuNPs_CIN. Moreover, ICP-OES was used to determine the wt % of Si and Au loading (ICP-OES, Thermo Scientific, iCAP7400DUO). The surface atomic composition was investigated using X-ray photoelectron spectroscopy (XPS) (Thermo Scientific, NEXSA). To gain further insight into the chemical bonding situation, the samples were analyzed using an FT-IR spectrometer equipped with an attenuated total reflector (ATR) mode, in the range of 4000–400 cm^{-1} with a resolution of 4.0 and a scan rate of 32 scans. Additionally, the optical properties of the fabricated papers were monitored between 200 and 800 nm by DRS (PerkinElmer, LAMBDA 950).

2.3. Antimicrobial Activity. WFY generated by various conditions such as pH, temperature, and oxygen contact during fermentation and storage of kimchi adversely affect the quality of kimchi by producing an off-odor and texture softening. To assess the antimicrobial activities of various functionalized papers, three types of WFY strains, which are present in the later stages of kimchi fermentation, were used. These included *C. sake* (MGB0659), *K. servazzii* (MGB0660), and *P. kudriavzevii* (MGB1001). Prior to the experiment, the stock strains of WFY were cultured in YPD broth at 25 °C for 24 h and subcultured three times to introduce healthy strains. As a result, three strain concentrations were obtained. Accordingly, one strain was inoculated directly onto a YPD agar plate, while the other two strains were inoculated on soft agar. Subsequently, these were diluted 10 times and 100 times, respectively, and then spread onto a YPD agar plate to allow the growth of yeast colonies. The control, Paper_AuNPs, Paper_CIN, and Paper_AuNPs_CIN samples were then placed on agar plates inoculated with each concentration of the strain and incubated at 24 °C for 48 to 72 h. The anti-yeast activities were evaluated by measuring the clear zone that formed around each sample after yeast expression. Additionally, the diameter of samples within the clear zone was disregarded during measurement.

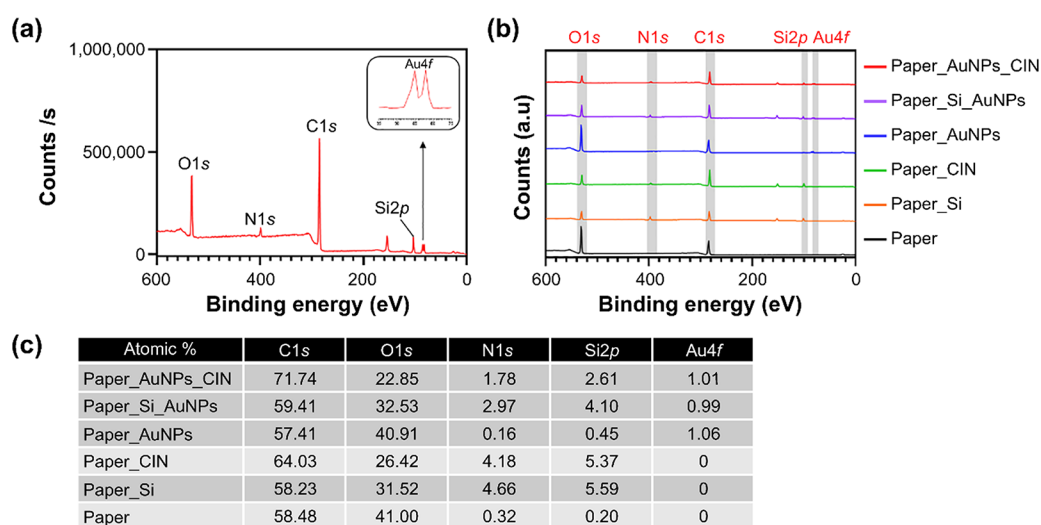


Figure 2. (a) XPS spectrum of the Paper_AuNPs_CIN film and narrow scan of Au4f (inset), (b) stacked XPS spectra, and (c) atomic composition percentages of films for each stage of fabrication.

3. RESULTS AND DISCUSSION

3.1. Fabrication and Characterization of Functionalized Films. The Paper_AuNPs_CIN film was manufactured using the three steps outlined in Scheme 1, which are as follows. In the first step, AuNPs are formed on the surface of the filter paper by reducing Au³⁺ (HAuCl₄) to Au⁰ in NaBH₄ aqueous solution, as indicated by a color change from white to purple in the filter paper. Moreover, lignin, a component of cellulose, acted synergistically with NaBH₄ to reduce gold ions.¹² The second step involved grafting APTES onto the surface of Paper_AuNPs to amine functionalization. APTES forms Si–O–C bonds with the surface, allowing it to react with one, two, or three –OH groups of the cellulose structure.¹³ Polarity affects the performance of functionalization because APTES forms intermolecular hydrogen bonds in polar solvents such as water and ethanol. In contrast, in toluene, the hydrogen bond between APTES molecules is weak, resulting in a greater potential for APTES molecules to react with the surface and a higher surface functionalization yield.¹⁴ Based on imine chemistry, the final step involves using the surface amines of Paper_Si_AuNPs in a condensation reaction with the aldehyde group of CIN in the presence of ethanol to form an imine linkage.^{15,16} Although AuNPs and CIN have been used separately in many studies, such as antimicrobial,^{7,8} catalyst,^{17,18} and packaging,¹⁹ to the best of our knowledge, this is the first report to confirm a synergistic antimicrobial effect of the AuNPs/CIN combination film. The fabrication of the Paper_CIN film followed the same procedure with the exception of the Paper_AuNPs step (Scheme 2).

Using SEM, the size, shape, and distribution of AuNPs on the Paper_AuNPs_CIN film were determined (Figure 1). On the cellulose surface, the produced AuNPs were spherically monodispersed with an average diameter of 46.8 ± 9.3 nm [Figure 1a]. Energy-dispersive spectroscopy (EDS) coupled with elemental mapping was utilized to determine the elemental identification, distribution, and quantitative analysis of the Paper_AuNPs_CIN film [Figure 1b]. The major components of the raw filter paper, C and O, were determined to be 66.06 and 31.13 wt %, respectively. There are two additional Si and Au peaks with 1.67 and 1.14 wt %,

respectively. Si atoms were introduced during APTES grafting onto the paper, and the presence of Au indicates the formation of AuNPs since unreacted Au ions were removed during rinsing. The specific compositions of Si and Au in the Paper_AuNPs_CIN film were determined using ICP-OES. The measured values for Si and Au were 1.8 and 1.2 wt %, respectively, which matched the EDS analysis values.

XPS was used to obtain more information about the bonding arrangement and atomic composition of the fabricated films and bare filter paper (Figure 2). Four binding energy peaks at 285.16, 532.4, 399.08, and 102.89 eV, corresponding to C1s, O1s, N1s, and Si2p, respectively, come from the paper, APTES, and CIN component, indicating that APTES and CIN molecules were functionalized on the paper surface [Figure 2a]. However, the double peaks at 85.88 and 82.28 eV, corresponding to Au4f, confirm the existence of zero-valence gold (Au⁰), which indicates a successful reduction of Au³⁺ ions to AuNPs on the surface (Figure 2a, inset). The XPS spectra are presented together (stacked on the same chart) to monitor the surface bonding in each fabrication process of the Paper_AuNPs_CIN and Paper_CIN films [Figure 2b]. When APTES was functionalized, a new Si2p peak appeared and the N1s peak was increased. Notably, the Si2p and Au4f peaks were newly generated by APTES surface functionalization and AuNPs reduction, respectively. In addition, it was shown that the size of the C1s peak increased compared to the O1s peak as the CIN molecules were bound to the surface. The atomic composition ratio of C, O, N, Si, and Au was measured at each fabrication step [Figure 2c]. The change in atomic composition showed the same trend as the peak changes in binding energy. Moreover, the amount of loaded CIN molecules could be calculated through a combination of atomic composition and comparison of film weights before (Paper_Si and Paper_Si_AuNPs) and after (Paper_CIN and Paper_AuNPs_CIN) CIN molecule bonding. Paper_AuNPs_CIN and Paper_CIN films were loaded with CIN molecules in the amounts of 632 and 413 μmol, respectively. The greater number of CIN molecules on the Paper_AuNPs_CIN film is caused by both the adsorption with AuNPs and chemical reactions.

ATR-FT-IR spectroscopy was utilized to elucidate the modification process of filter paper with APTES and the

subsequent surface functionalization with CIN (Figure 2). There was no significant difference in the spectrum between bare filter paper (black) and Paper_AuNPs (blue), while the signature peaks at 1562 and 1475 cm^{-1} of Paper_Si (orange) were attributed to symmetric NH_3^+ deformation and NH_2 bending of APTES, respectively.^{9,14} The fabrication of the Paper_CIN and the Paper_AuNPs_CIN is based on the Schiff base reaction between the amino group of APTES and the aldehyde group of CIN.¹⁵ In the spectrum of Paper_CIN (green), the disappearance of the NH_2 and NH_3^+ peaks and the formation of an additional $\text{C}=\text{N}$ bond at 1635 cm^{-1} indicate that surface functionalization with CIN was successful. It should be noted that Paper_AuNPs_CIN (red) exhibited a distinct peak at 1680 cm^{-1} , which can be attributed to aldehyde ($\text{C}=\text{O}$) adsorbed on the AuNPs surface.¹⁶ Owing to the physical adsorption of CIN and AuNPs, in addition to the Schiff base reaction, it is possible to produce a functionalized film with a higher concentration of CIN on its surface. Optical properties of the as-prepared bare and functionalized films were monitored using UV-vis DRS because they exhibited a distinct absorption band that can be used to characterize the presence of a compound at specific wavelengths.¹⁷ The peak of Paper_AuNPs (blue) and Paper_AuNPs_CIN (red) at 530 nm was a localized surface plasmon resonance (LSPR) peak that could be expected from spherical AuNPs with a size of 50 nm, which corresponded to the size of AuNPs observed by SEM (Figure 1).¹⁸ The maximum absorbance of CIN at 290 nm coincided with a previously reported peak of *trans*-cinnamaldehyde (Figure 3).¹⁹ The FT-IR and DRS results demonstrated that AuNPs, APTES, and CIN were successfully grafted onto the paper surface (Figure 4).

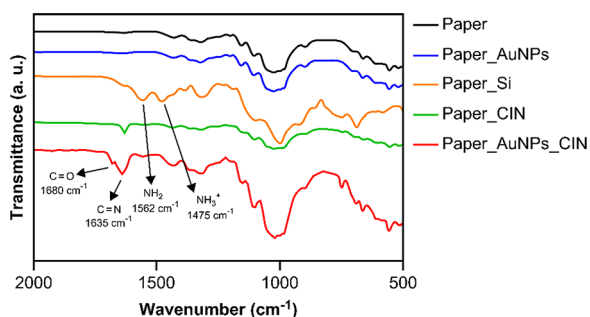


Figure 3. FT-IR (ATR mode) spectra of raw filter paper and functionalized films.

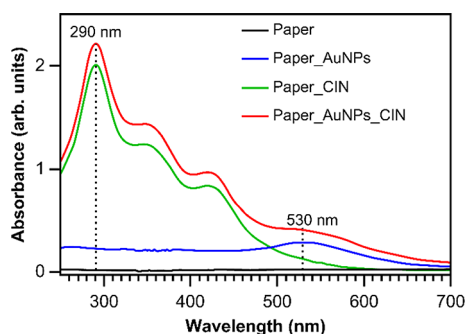


Figure 4. UV-vis DRS of raw filter paper, Paper_AuNPs, Paper_CIN, and Paper_AuNPs_CIN.

3.2. Antimicrobial Activity against Three Types of WFY. WFY produced during fermentation and storage of

kimchi reduces the quality of kimchi by its distinct off-odor and texture softening; therefore, its growth must be prevented. *C. sake* [Figure 5a], *P. kudriavzevii* [Figure 5b], and *K. servazzii* [Figure 5c] strains that produce WFY during the fermentation of kimchi were used to test the antimicrobial activities of functionalized films using the agar-well diffusion method (Figure 5). In all introduced WFY strains, functionalized films with CIN affected growth kinetics differed from the Paper_AuNPs and untreated filter paper (control). In the order of Paper_AuNPs_CIN and Paper_CIN, the inhibition zone was 12.9 ± 0.4 and 7.7 ± 0.6 mm in *C. sake*, 12.2 ± 0.5 and 8.0 ± 0.5 mm in *P. kudriavzevii*, and 6.8 ± 0.3 and 3.2 ± 0.4 mm in *K. servazzii*, respectively. In the same experiments, diluting each strain by a factor of 100 had no discernible effect. This is attributable to the interaction of CIN with the hydrophobic structure of the bacterial cell membrane, resulting in impaired cell membrane permeability and integrity.²⁰ Previous studies demonstrated that AuNPs with a size of less than 20 nm inhibited the growth of *Escherichia coli* and *Pseudomonas aeruginosa* and exhibited antimicrobial effects; however, Paper_AuNPs with a size of 46.8 nm exhibited no antimicrobial activity against three types of WFY.^{10,21} In contrast, when both AuNPs and CIN were present, the highest antimicrobial activity was observed. AuNPs were formed on the surface of the filter paper to enhance its antimicrobial activity because a larger quantity of antimicrobials can be adsorbed onto the AuNPs surface, owing to the high adsorption affinity of nanoparticles with a large surface area.¹³ Furthermore, owing to the adsorption affinity between AuNPs and CIN molecules, additional CIN molecules were present on the film surface besides the CIN bound via the imine reaction, resulting in the highest antimicrobial activity in the Paper_AuNPs_CIN film.¹⁶ There have been studies on suppressing WFY by directly spraying cinnamon and garlic extracts onto kimchi. However, when high concentrations of extracts are used to increase the antimicrobial effect, the sensory properties are affected by the strong odor and flavor properties of cinnamon and garlic.⁷ In this study, since CIN was adsorbed and chemically bound to the film surface via AuNPs adsorption and imine reaction, respectively, it was anticipated that it would act as a WFY inhibitor in kimchi without affecting the sensory properties.

4. CONCLUSIONS

In this study, an antimicrobial film for use against WFY was successfully fabricated and tested. AuNPs were formed on the surface of the filter paper, and the antimicrobial agent, CIN, was immobilized by imine bonding and adsorption. SEM images confirmed the spherical shape and uniform distribution of the AuNPs on the paper's surface, while EDS and ICP-OES analyses determined their elemental ratio. Each synthesis step, in which CIN molecules were imine-bonded and adsorbed to the surface of the paper and AuNPs, respectively, was confirmed by FT-IR analysis. By measuring the DRS of the fabricated films and identifying a peak of specific functional groups, the optical properties of each used material were determined. In order to apply this, the antimicrobial activities of WFY strains generated under different fermentation and storage conditions of kimchi were evaluated using the agar-well diffusion assay. In particular, the Paper_AuNPs_CIN film exhibited the largest inhibition zone and the highest antimicrobial activity against three types of WFY: *C. sake*, *P. kudriavzevii*, and *K. servazzii*. Our functionalized antimicrobial

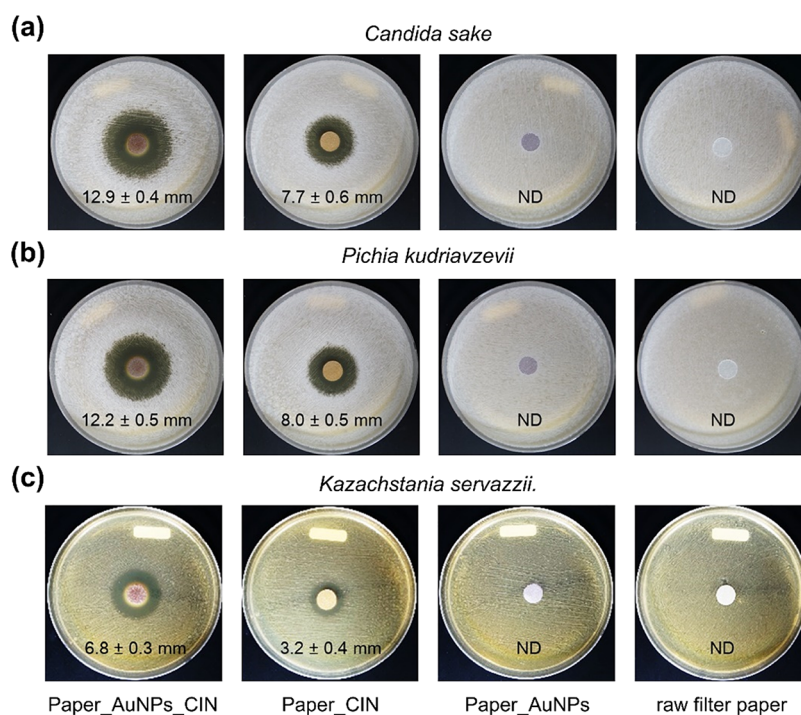


Figure 5. Test and measurement of the inhibition zones of Paper_AuNPs_CIN, Paper_CIN, Paper_AuNPs, and raw filter paper (control) against three types of WFY: (a) *C. sake*, (b) *P. kudriavzevii*, and (c) *K. servazzii*. ND: not detectable.

film, the Paper_AuNPs_CIN film, can extend the shelf-life without altering sensory properties, even when in contact with kimchi, owing to the chemical bonding and adsorption of antimicrobial-agent CIN molecules to the film surface. Furthermore, the transportation and distribution of kimchi take a long time, especially during export. During this period, WFY are generated on the surface of kimchi, which prompts complaints from consumers and leads to a financial loss to the industry. Our research results indicate that the inhibitory effect of our Paper_AuNPs_CIN films against WFY of kimchi should effectively reduce the issues associated with the time-consuming transportation and distribution. In the long run, it is anticipated that additional research on this strategy will prevent the deterioration of the quality of distributed kimchi by extending its storage stability and shelf-life.

AUTHOR INFORMATION

Corresponding Author

Sung Gi Min – World Institute of Kimchi, Gwangju 61755, Republic of Korea; orcid.org/0000-0002-6461-0823; Phone: +82-62-610-1806; Email: skmin@wikim.re.kr; Fax: +82-62-610-1850

Authors

Seong Youl Lee – World Institute of Kimchi, Gwangju 61755, Republic of Korea

Eun Hae Kim – World Institute of Kimchi, Gwangju 61755, Republic of Korea

Tae-Woon Kim – World Institute of Kimchi, Gwangju 61755, Republic of Korea

Young-Bae Chung – World Institute of Kimchi, Gwangju 61755, Republic of Korea

Ji-Hee Yang – World Institute of Kimchi, Gwangju 61755, Republic of Korea

Sung Hee Park – World Institute of Kimchi, Gwangju 61755, Republic of Korea; orcid.org/0000-0003-0752-0730

Mi-Ai Lee – World Institute of Kimchi, Gwangju 61755, Republic of Korea; orcid.org/0000-0001-7131-9703

Complete contact information is available at:

<https://pubs.acs.org/10.1021/acsomega.2c06323>

Notes

The authors declare no competing financial interest.

ACKNOWLEDGMENTS

This research was supported by the WIKIM Research Program (KE2203-1) through the World Institute of Kimchi, funded by the Ministry of Science, ICT, and Future Planning, Republic of Korea.

REFERENCES

- (1) Lee, M. A.; Choi, Y. J.; Lee, H.; Hwang, S.; Lee, H. J.; Park, S. J.; Chung, Y. B.; Yun, Y.-R.; Park, S.-H.; Min, S.; Kwon, L.-S.; Seo, H.-Y. Influence of Salinity on the Microbial Community Composition and Metabolite Profile in Kimchi. *Fermentation* **2021**, *7*, 308.
- (2) (a) Kim, J. Y.; Kim, J.; Cha, I.-T.; Jung, M. Y.; Song, H. S.; Kim, Y. B.; Lee, C.; Kang, S.-Y.; Bae, J.-W.; Choi, Y.-E.; Kim, T.-W.; Roh, S. W. Community structures and genomic features of undesirable white colony-forming yeasts on fermented vegetables. *J. Microbiol.* **2019**, *57*, 30–37. (b) Moon, S. H.; Chang, M.; Kim, H. Y.; Chang, H. C. *Pichia kudriavzevii* is the major yeast involved in film-formation, off-odor production, and texture-softening in over-ripened Kimchi. *Food Sci. Biotechnol.* **2014**, *23*, 489–497.
- (3) Kim, M.-J.; Lee, H.-W.; Kim, J. Y.; Kang, S. E.; Roh, S. W.; Hong, S. W.; Yoo, S. R.; Kim, T.-W. Impact of fermentation conditions on the diversity of white colony-forming yeast and analysis of metabolite changes by white colony-forming yeast in kimchi. *Food Res. Int.* **2020**, *136*, No. 109315.
- (4) (a) Navani, N. K.; Ghosh; Deepak, P.; Sharma, T.; Srivastava; Pathania, R. Synergistic action of cinnamaldehyde with silver

- nanoparticles against spore-forming bacteria: a case for judicious use of silver nanoparticles for antibacterial applications. *Int. J. Nanomed.* **2013**, *4721*. (b) Adams, T. B.; Cohen, S. M.; Doull, J.; Feron, V. J.; Goodman, J. I.; Marnett, L. J.; Munro, I. C.; Portoghese, P. S.; Smith, R. L.; Waddell, W. J.; Wagner, B. M. The FEMA GRAS assessment of cinnamyl derivatives used as flavor ingredients. *Food Chem. Toxicol.* **2004**, *42*, 157–185.
- (5) (a) Warnke, P. H.; Becker, S. T.; Podschun, R.; Sivanathan, S.; Springer, I. N.; Russo, P. A. J.; Wiltfang, J.; Fickenscher, H.; Sherry, E. The battle against multi-resistant strains: Renaissance of antimicrobial essential oils as a promising force to fight hospital-acquired infections. *J. Cranio-Maxillofac. Surg.* **2009**, *37*, 392–397. (b) Burt, S. Essential oils: their antibacterial properties and potential applications in foods—a review. *Int. J. Food Microbiol.* **2004**, *94*, 223–253.
- (6) (a) Bilbao-Sainz, C.; Chiou, B.-S.; Du, W.-X.; Gregorsky, K. S.; Orts, W. J. Influence of Disperse Phase Characteristics on Stability, Physical and Antimicrobial Properties of Emulsions Containing Cinnamaldehyde. *J. Am. Oil Chem. Soc.* **2013**, *90*, 233–241. (b) Chen, H.; Davidson, P. M.; Zhong, Q. Impacts of Sample Preparation Methods on Solubility and Antilisterial Characteristics of Essential Oil Components in Milk. *Appl. Environ. Microbiol.* **2014**, *80*, 907–916.
- (7) Kim, M.-J.; Kang, S.-E.; Jeong, C. H.; Min, S.-G.; Hong, S. W.; Roh, S. W.; Jhon, D.-Y.; Kim, T.-W. Growth Inhibitory Effect of Garlic Powder and Cinnamon Extract on White Colony-Forming Yeast in Kimchi. *Foods* **2021**, *10*, 645.
- (8) Ramasamy, M.; Lee, J.-H.; Lee, J. Direct one-pot synthesis of cinnamaldehyde immobilized on gold nanoparticles and their antibiofilm properties. *Colloids Surf, B* **2017**, *160*, 639–648.
- (9) (a) Murphy, C. J.; Sau, T. K.; Gole, A. M.; Orendorff, C. J.; Gao, J.; Gou, L.; Hunyadi, S. E.; Li, T. Anisotropic Metal Nanoparticles: Synthesis, Assembly, and Optical Applications. *J. Phys. Chem. B* **2005**, *109*, 13857–13870. (b) Ashraf, S.; Pelaz, B.; del Pino, P.; Carril, M.; Escudero, A.; Parak, W. J.; Soliman, M. G.; Zhang, Q.; Carrillo-Carrion, C. Gold-Based Nanomaterials for Applications in Nanomedicine. In *Light-Responsive Nanostructured Systems for Applications in Nanomedicine*, Sortino, S. Ed.; Springer International Publishing, 2016; pp. 169–202.
- (10) (a) Musikavanhu, B.; Hu, Z.; Dzapata, R. L.; Xu, Y.; Christie, P.; Guo, D.; Li, J. Facile method for the preparation of superhydrophobic cellulosic paper. *Appl. Surf. Sci.* **2019**, *496*, No. 143648. (b) Li, H.; He, Y.; Yang, J.; Wang, X.; Lan, T.; Peng, L. Fabrication of food-safe superhydrophobic cellulose paper with improved moisture and air barrier properties. *Carbohydr. Polym.* **2019**, *211*, 22–30.
- (11) Zille, A.; Almeida, L.; Amorim, T.; Carneiro, N.; Esteves, M. F.; Silva, C. J.; Souto, A. P. Application of nanotechnology in antimicrobial finishing of biomedical textiles. *Mater. Res. Express* **2014**, *1*, No. 032003.
- (12) Bumbudsanpharoke, N.; Ko, S. PEER-REVIEWED ARTICLE In-situ Green Synthesis of Gold Nanoparticles using Unbleached Kraft Pulp. *BioResources* **2015**, *10*, 6428–6441.
- (13) He, W.; Zhang, Z.; Zheng, Y.; Qiao, S.; Xie, Y.; Sun, Y.; Qiao, K.; Feng, Z.; Wang, X.; Wang, J. Preparation of aminoalkyl-grafted bacterial cellulose membranes with improved antimicrobial properties for biomedical applications. *J. Biomed. Mater. Res., Part A* **2020**, *108*, 1086–1098.
- (14) Munguia, C. L.; Perez, H. I.; Ojeda, L. R.; Esparza, S. J. M.; Dominguez, O. A.; Felipe, M. C.; Cervantes, U. A. APTES-functionalization of Sba-15 using ethanol or toluene: textural characterization and sorption performance of carbon dioxide. *J. Mex. Chem. Soc.* **2017**, *61*, 273–281.
- (15) Ramasamy, M.; Lee, J.-H.; Lee, J. Development of gold nanoparticles coated with silica containing the antibiofilm drug cinnamaldehyde and their effects on pathogenic bacteria. *Int. J. Nanomed.* **2017**, *Volume 12*, 2813–2828.
- (16) Cionti, C.; Taroni, T.; Sabatini, V.; Meroni, D. Nanostructured Oxide-Based Systems for the pH-Triggered Release of Cinnamaldehyde. *Materials* **2021**, *14*, 1536.
- (17) Zheng, G.; Polavarapu, L.; Liz-Marzán, L. M.; Pastoriza-Santos, I.; Pérez-Juste, J. Gold nanoparticle-loaded filter paper: a recyclable dip-catalyst for real-time reaction monitoring by surface enhanced Raman scattering. *Chem. Commun.* **2015**, *51*, 4572–4575.
- (18) Goyal, D.; Saini, A.; Saini, G. S. S.; Kumar, R. Green synthesis of anisotropic gold nanoparticles using cinnamon with superior antibacterial activity. *Mater. Res. Express* **2019**, *6*, No. 075043.
- (19) Cui, R.; Yan, J.; Cao, J.; Qin, Y.; Yuan, M.; Li, L. Release properties of cinnamaldehyde loaded by montmorillonite in chitosan-based antibacterial food packaging. *Int. J. Food Sci. Technol.* **2021**, *56*, 3670–3681.
- (20) Meroni, D.; Lo Presti, L.; Di Liberto, G.; Ceotto, M.; Acres, R. G.; Prince, K. C.; Bellani, R.; Soliveri, G.; Ardzzone, S. A Close Look at the Structure of the TiO₂-APTES Interface in Hybrid Nanomaterials and Its Degradation Pathway: An Experimental and Theoretical Study. *J. Phys. Chem. C* **2017**, *121*, 430–440.
- (21) Wong, M.-Y.; Amini Horri, B.; Salamatinia, B. Grafted Copolymerized Chitosan and Its Applications as a Green Biopolymer. In *Biopolymer Grafting*, Thakur, V. K. Ed.; Elsevier, 2018, pp. 285–333.